Generation of binary and multicomponent metal nanoparticles and carbon-coated nanoparticles by electrical explosion of wires

Zekun Yin , Jian Wu , Liwen Liang , Chuncai Kong , Huantong Shi and Xingwen Li

State Key Laboratory of Electrical Insulation and Power Equipment, Xi'an Jiaotong University, No. 28 XianNing West Road, Xi'an, Shaanxi Province 710049, China

Abstract: Electrical explosion of wires (EEW) has been an efficient method to prepare nanoparticles, and nanoparticles with different structure and composition can be produced by twisting metal wires or combining metal wires with different materials by electric explosion. In this paper, binary and multicomponent metal nanoparticles and carbon-coated aluminum nanoparticles are prepared by EEW. The morphology, composition and structure of nanoparticles are analyzed by Field Emission Transmission Electron Microscope (FE-TEM), X-Ray Diffraction (XRD), Energy Dispersion Spectrum (EDS) line scans and element mapping.

Keywords: electrical explosion of wires, nanoparticles

1. Introduction

The EEW is widely used in various fields of science and technology, such as Z-pinch [1], shock wave generation [2], production of nanoparticles, etc. Due to high efficiency and yield, low energy consumption and high purity, the EEW has become a promising way to prepare nanoparticles [3]. The EEW is based on pulse discharge technology, which causes the energy storage on the capacitor to be released to the wire in a short time, and the wire is instantaneously vaporized to form nanoparticles. When a high density current flows through the wire, the injected ohmic energy heats the wire, the wire experiences a phase transition of melting, vaporization, and plasma in an instant. As a result, the wire is turned into gaseous or plasma column, which cools down as it expands into the surrounding gas and eventually forms nanoparticles [4]-[6].

In this paper, binary and multicomponent metal nanoparticles and carbon-coated aluminum nanoparticles are prepared by EEW. The morphology, composition and structure of nanoparticles are analyzed by Field Emission Transmission Electron Microscope (FE-TEM), X-Ray Diffraction (XRD), Energy Dispersion Spectrum (EDS) line scans and element mapping.

2. Experimental Method

2.1. Binary and multicomponent metal nanoparticles

Metal materials for producing bimetallic nanoparticles can be basically divided into two groups: one is the metal with low melting and boiling point, including Cu, Ag, Al, and the other is the metal with high melting and boiling point, including W, Ti, Ni etc [7]. Binary and multicomponent metal nanoparticles are prepared by electric explosion of two or more twisted wires as shown in Figure 1. The EEW system is shown in Reference 18. The diameter and length of Al wire and Cu wire used to prepare binary metal nanoparticles are 0.2mm and 8cm respectively, and the metal wires used to prepare polymetallic nanoparticles are shown in Table 1.

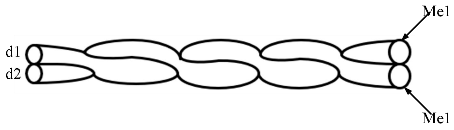

Fig. 1. The structure of the two twisted wires

Table 1. The Wire characteristics used to prepare multicomponent metal nanoparticles.

Sample	Wire metals	d/mm	l/cm	n/%	C/μF	U/kV
1	Fe	0.3	7.5	27.1	4	30
	Mo	0.2	7.5	9.1		
	Cu	0.3	7.5	27.0		
	Ti	0.2	7.5	8.1		
	$Ni_{78}Cr_{22}$	0.3	7.5	Ni-21.8 Cr-6.9		
2	Fe	0.3	7.5	17.9	4	30
	Mo	0.2	7.5	6.0		
	Cu	0.4	7.5	31.6		
	Ti	0.2	7.5	5.3		
	Al	0.2	7.5	5.6		
	$Ni_{78}Cr_{22}$	0.4	7.5	Ni-25.5 Cr-8.1		

2.2. Carbon-coated Al nanoparticles

The aluminum wire is evenly spirally wound on a graphite rod with a diameter of 1 mm and a length of 8 cm. The aluminum wire is 0.25 mm in diameter and a total length of 10 cm as shown in Figure 2. The above load is fixed between the upper and lower electrodes of the electric explosion chamber for the electric explosion experiment and the product nanoparticles are collected for characterization.

Fig. 2. The structure of the load used to produce carbon-coated nanoparticles

3. Results and Discussion

3.1. Binary and multicomponent metal nanoparticles

The typical morphology of the Cu/Al nanoparticles under different charging voltages is presented in Fig.3. It can be found that almost all the Cu/Al nanoparticles are basically spherical in shape. Very few particles that are much larger are present under the 20kV charging voltage. There is no obvious formation of particles separated into an individual component in the particles, so the elements in the particles should be homogenous distributed. The nanoparticles produced under these four conditions may consist of high Al content relative to Cu or high Cu content relative to Al. The analysis of the structure and elements are shown in Fig.4. The inside of the nanoparticles is rich in Al and Cu, but the surface of the nanoparticles with core-shell structure only contains Al.

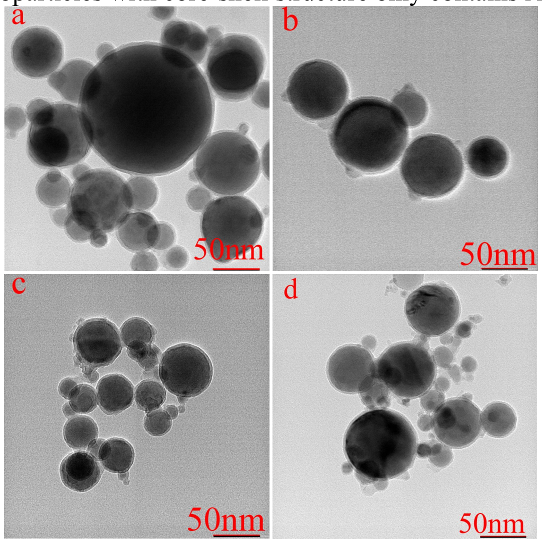

Fig. 3. Typical morphology of the Cu/Al nanoparticles under differentcharging voltages. (a) 20kV. (b) 25kV (c) 30kV (d) 40kV

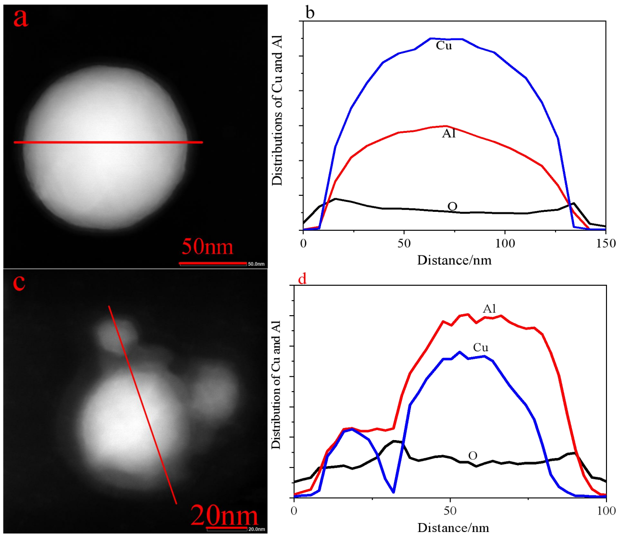

Fig. 4. The structure and elements of the Cu/Al nanoparticles (a) EDS line scans (b) Particles with uniformly distributed structure (c) EDS line scans (d) Particles with core-shell structure

In order to investigate the composition of the nanoparticles, the element mapping of a number of single nanoparticles is used shown in Fig.5. It is clear that the particles are characterized by a homogenous distribution of Cu and Al components throughout the volume. The melting point of Cu and Al is similar, the deposited energy in the wire is enough to make the Cu and Al melt together in the melting stage, so that the Cu and Al are evenly distributed. The surface layer of some Cu/Al bimetallic nanoparticles is Al of several nanometers, that is, the Cu is coated with a layer of Al. It may be that the specific density and melting point of Al are lower than that of Cu, which results in the movement of Al to the periphery of the particles and the formation of a layer of Al on the surface of the bimetallic nanoparticles.

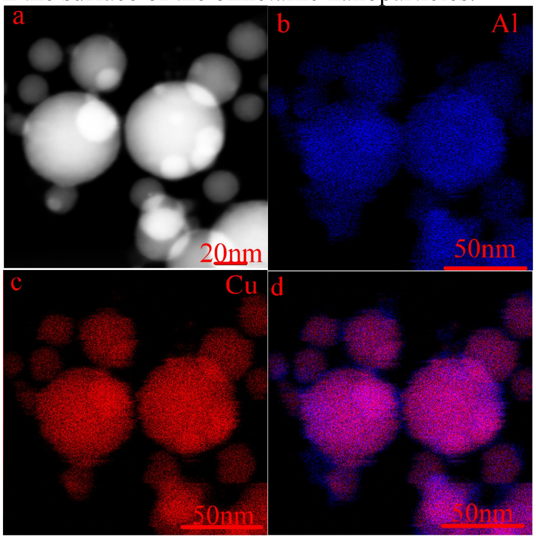

Fig. 5. The element mapping of a number of single nanoparticles

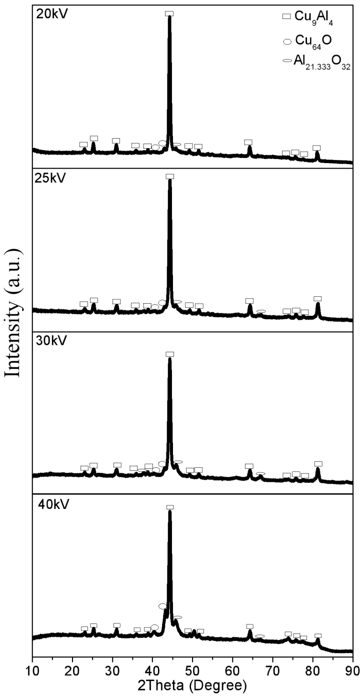

Fig. 6. Data of the X-ray diffraction analysis of the Cu/Al nanoparticles under different charging voltages

Fig. 6 shows the results of XRD results of the Cu/Al nanoparticles. All analyzed nanoparticles include copper oxides $Cu_{64}O$, aluminum oxides $Al_{21.333}O_{32}$, and the solid solution of Cu shows that the lattice parameter of Cu_9Al_4 is 8.703 ± 0.01Å, and no solid solution based on Al is found in the sample. As the voltage increases, it is clear at 40kV that the strength of the Cu oxides and Al oxides in the sample increases. The deposited energy in the wire increases with the increase of charging voltage, which causes the copper-based solid solution to dissolve, thereby forming more Cu oxides and Al oxides. And the oxide content in all samples is very low.

Table 2. The parameters of multicomponent alloy.

Parameters	Sample1	Sample2
δ(%)	4.94	4.97
ΔH_{mix}(kJ/mol)	0.78	-0.34
ΔS_{mix}[J/(mol • K)]	13.68	14.22
VEC	8.6	8.7

HEA tends to form simple solid solution structures, such as face-centered cubic (fcc) or body-centered cubic (bcc) or a mixture of both [8]. At present, the prediction of high entropy alloy structure is mainly based on the difference of atomic radius (δ), Enthalpy of mixing (ΔH_{mix}), mixing entropy (ΔS_{mix}) valence electron concentration (VEC) and other parameters are considered, however, there is still controversy about the range of the above values of the HEA structural phase [9]. The research work (16) pointed out that the hard sphere model can be used to predict the crystal structure of HEA. According to the model, at $-15<\Delta H_{mix}<10$ kJ/mol and $0<\delta<5\%$, the formed high entropy alloy is single-phase solid solution. At $-20<\Delta H_{mix}<0$ kJ/mol and $5<\delta<8\%$, forming multiphase solid solution. The research work [10] pointed out that the solid solution based on fcc lattice was formed at $VEC\geq 8.0$, and the solid solution based on bcc lattice was formed at $VEC\leq 6.87$.

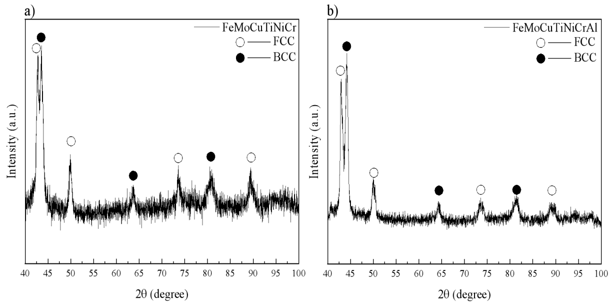

Fig. 7. Data of the X-ray diffraction analysis of the multicomponent metal nanoparticles. (a) FeMoCuTiNiCr (b) FeMoCuTiNiCrAl

Fig. 7 shows the XRD results of six-component and seven-component metal nanoparticles. Both samples are two-phase solid solutions with FCC and BCC structures. Table 2 shows the parameter values of atomic radius difference, mixing enthalpy, mixing entropy and valence electron concentration of the two samples. According to the values in the table and the prediction range described above, the two samples should be single-phase solid solution structure in theory, but actually two-phase mixed solid solution structure. The reason for this is that the determination of the parameter range is controversial at first, and the difference of atomic radii of the two samples is near the critical value, resulting in greater uncertainty [11].

3.2. Carbon-coated Al nanoparticles

The TEM image of carbon-coated aluminum nanoparticles prepared by electric explosion experiment with aluminum wire and graphite rod is shown in Fig. 8. It can be seen from the figure that the nanoparticles are basically spherical, and there is no obvious agglomeration phenomenon.

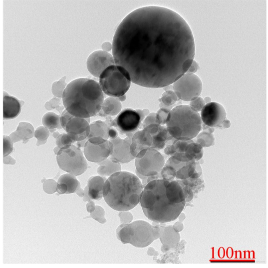

Fig. 8. TEM images of carbon-coated nanoparticles

At the same time, EDS was also used to analyze the element distribution of carbon-coated aluminum nanoparticles. The line scan results of typical carbon-coated aluminum nanoparticles are shown in Fig. 9. It can be seen from the figure that the result of line scanning is basically the same as that of carbon-coated aluminum nanoparticles prepared by the electric explosion experiment of aluminum wire and carbon tube. The core of the nanoparticles is mainly composed of aluminum, while the carbon is mainly coated on the surface of the particles. For the particles with diameters of about 35 nm and 55 nm, the carbon layer thickness is about 2 nm and 3 nm.

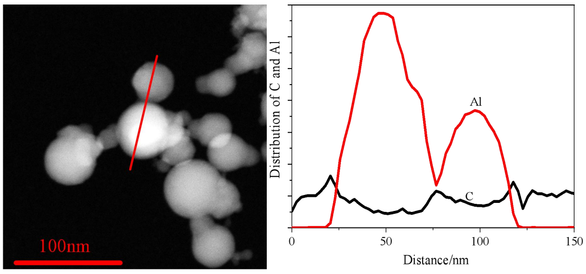

Fig. 9. EDS line scans of carbon-coated aluminum nanoparticles

At the same time, surface scanning is used to observe different areas of the sample, and it can be seen that the collected nanoparticles have carbon layers, as shown in Fig. 10. The red color in the figure represents Al, and the green color represents C. It can be determined that the carbon-coated nanoparticles prepared by the electric explosion experiment with aluminum wire and graphite rod have a high proportion of carbon coating.

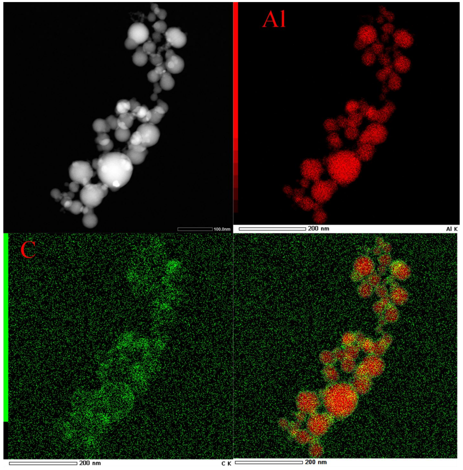

Fig. 10. The element mapping of carbon-coated aluminum nanoparticles

The typical XRD diffraction images of carbon-coated nanoparticles made from aluminum wire and graphite rod are shown in Fig. 11. It can be seen that almost no Al oxide phase is found in these carbon-coated Al nanoparticles, which indicates that the carbon layer has the ability to effectively prevent Al oxidation. Although Al carbide phase was found in these carbon-coated Al nanoparticles, its content was very low. It can be considered that most of the Al microcrystals wrapped in the core of the carbon shell were ordinary metal phases.

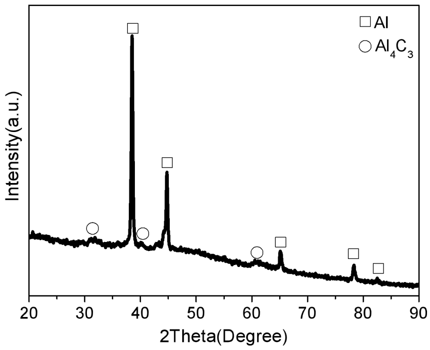

Fig. 11. Data of the X-ray diffraction analysis of the carbon-coated nanoparticles

4. Summary

Binary and multicomponent metal nanoparticles and carbon-coated aluminum nanoparticles were prepared by electric explosion of metal wires. The main conclusions are summarized as follows:

(1) With the change of charging voltage, the crystal phase in the binary metallic nanoparticles remained basically unchanged.

(2) The solid solution formed by multi-component metal nanoparticles obtained by electric explosion of metal wire is two-phase solid solution. To obtain single-phase solid solution, it may be necessary to accelerate the cooling rate of metal vapor.

(3) The carbide content of Al in the carbon-coated Al nanoparticles is very low. It can be considered that most of the Al microcrystals wrapped in the core of the carbon shell are ordinary metal phases.

5. References

[1] Jian Wu, Xingwen Li, Mo Li, Yang Li and Aici Qiu, Journal of Physics D Applied Physics, **50,** (2017).

[2] G. S. Sarkisov, J. Caplinger, F. Parada, and V. I. Sotnikov, Journal of Applied Physics, **123,** 123303 (2016).

[3] H. Suematsu, K. Murai, Y. Tokoi, T. Suzuki, T. Nakayama, W. Jiang, and K. Niihara, Journal of the Chinese Ceramic Society, **35,** 939-947 (2007).

[4] Shi Huantong, Wu Jian, Li Xingwen, Murphy A B, Li Xudong, Chen Li and Li Penghui, Plasma Sources Science and Technology, **28,** (2019).

[5] Xudong Li, Huantong Shi, Chaopeng Liu, Jian Wu, Li Chen, Shaojun Qiu, Xingwen Li and Aici Qiu, IEEE Transactions on Plasma Science, **47,** 1933-1938 (2019).

[6] T K Sindhu, R Sarathi and S R Chakravarthy, Nanotechnology, **19,** 025703 (2008).

[7] A. Pervikov, E. Glazkova, and M. Lerner, Physics of Plasmas, (2018).

[8] Tomboc, Gracita M., Taehyun Kwon, Jinwhan Joo and Kwangyeol Lee, Journal of Materials Chemistry, **8,** 14844-14862 (2020).

[9] George, Elizabeth P, William A. Curtin and Cemal Cem Tasan., Acta Materialia, **188,** 435-474 (2020).

[10] Guo, Sheng, Chun Ng, Jian Lu and C. T. Liu, Journal of Applied Physics, **109,** 103505 (2011).

[11] Suliz, K. V., Anderson Miller, Konstantin Ivanov and Aleksandr Pervikov, Powder Technology, (2022).